Transduction of Tumor-Specific T Cells with CXCR2 Chemokine Receptor Improves Migration to Tumor and Antitumor Immune Responses

Weiyi Peng[1], Yang Ye[1], Brian A. Rabinovich[2], Chengwen Liu[1], Yanyan Lou[1], Minying Zhang[1], Mayra Whittington[1], Yan Yang[1], Willem W. Overwijk[1], Gregory Lizée[1], and Patrick Hwu[1]

Abstract

Purpose: One of the most important rate-limiting steps in adoptive cell transfer (ACT) is the inefficient migration of T cells to tumors. Because melanomas specifically express the chemokines CXCL1 and CXCL8 that are known to facilitate the CXCR2-dependent migration by monocytes, our aim is to evaluate whether introduction of the *CXCR2* gene into tumor-specific T cells could further improve the effectiveness of ACT by enhancing T-cell migration to tumor.

Experimental Design: In this study, we used transgenic pmel-1 T cells, which recognize gp100 in the context of H-2Db, that were transduced with *luciferase* gene to monitor the migration of transferred T cells *in vivo*. To visualize luciferase-expressing T cells within a tumor, a nonpigmented tumor is required. Therefore, we used the MC38 tumor model, which naturally expresses CXCL1.

Results: Mice bearing MC38/gp100 tumor cells treated with CXCR2/luciferase-transduced pmel-1 T cells showed enhanced tumor regression and survival compared with mice receiving control luciferase-transduced pmel-1 T cells. We also observed preferential accumulation of CXCR2-expressing pmel-1 T cells in the tumor sites of these mice using bioluminescence imaging. A similar enhancement in tumor regression and survival was observed when CXCR2-transduced pmel-1 T cells were transferred into mice bearing CXCL1-transduced B16 tumors compared with mice treated with control pmel-1 T cells.

Conclusions: These results implicate that the introduction of the *CXCR2* gene into tumor-specific T cells can enhance their localization to tumors and improve antitumor immune responses. This strategy may ultimately enable personalization of cancer therapies based on chemokine expression by tumors. *Clin Cancer Res; 16(22); 5458–68. ©2010 AACR.*

Given the shown effectiveness of T cells in mediating antitumor immune responses, T-cell–mediated immunotherapy is considered an important and promising therapeutic approach against cancer. In particular, adoptive cell transfer (ACT) combined with lymphodepletion has resulted in clinical responses in ~50% to 70% of patients with metastatic melanoma (1, 2). However, the requirement of large numbers of laboratory-expanded T cells ($>1 \times 10^{10}$) makes ACT a costly and labor-intensive treatment. In addition, although some ACT patients achieve long-term disease-free survival, most patients still recur with disease (3). One important limiting factor for ACT is the inefficient migration of T cells into tumor tissue. By labeling T cells before ACT, it has been shown that the number of adoptively transferred T cells migrating to the tumor microenvironment correlates positively with clinical response (4). However, this analysis also showed that the trafficking efficiency of transferred T cells was extremely low (5). Therefore, strategies aimed at improving the migration of T cells to tumor sites are likely to enhance the efficacy of ACT therapy and improve clinical response rates.

Chemokines are secreted proteins that are essential for mediating the trafficking of immune cells to sites of inflammation. Through chemotaxis, cells that express appropriate chemokine receptors can migrate along a chemokine gradient to localize to specific tissues or sites of infection (6). Chemokines also play an important role in T-cell–mediated antitumor immune responses. For example, mice lacking CXCR6, the receptor for CXCL16, displayed reduced recruitment of activated effector T cells in breast tumor tissue and impaired tumor regression (7).

Authors' Affiliations: Departments of [1]Melanoma Medical Oncology and [2]Experimental Diagnostic Imaging, The Center for Cancer Immunology Research, The University of Texas M. D. Anderson Cancer Center, Houston, Texas

Note: Supplementary data for this article are available at Clinical Cancer Research Online (http://clincancerres.aacrjournals.org/).

Corresponding Author: Patrick Hwu, Department of Melanoma Medical Oncology, The Center for Cancer Immunology Research, The University of Texas M. D. Anderson Cancer Center, Unit 430, 1515 Holcombe Boulevard, Houston, TX 77030. Phone: 713-563-1728; Fax: 713-745-1046; E-mail: phwu@mdanderson.org.

©2010 American Association for Cancer Research.

American Association for **Cancer Research**

Translational Relevance

Adoptive T-cell therapy (ACT) has tremendous potential for the treatment of patients with advanced cancers, but a major limitation is the inefficient migration of T cells to the tumor site. In this study, we report our success in enhancing the migratory ability of T cell to tumors, further improving the antitumor immune response and survival in tumor-bearing mice in two distinct tumor models, by transduction of tumor-specific T cells with the gene encoding CXCR2. These results suggest that transducing CXCR2 into tumor-specific T cells provides an important avenue in "personalized cancer therapy" to take advantage of defined chemokine signatures within the tumor microenvironment, and is a significant step forward in the improvement of adoptive T-cell therapy. With these results, we planned to use the CXCR2 receptor in our ACT-based clinical trials in the next 2 years here at M. D. Anderson Cancer Center.

Affymetrix gene expression analysis of metastatic melanoma specimens has shown that the presence of T cells in tumor tissue is associated with high expression of many chemokines (8, 9), suggesting that their migration to tumors may be regulated by chemokines. Although the majority of human melanoma tumors show high levels of expression of CXCL1 and CXCL8 (10–12), the number of tumor antigen–specific T cells in these tumors is very limited (8, 13). However, melanoma tumors almost invariably show high levels of monocyte/macrophage infiltrates that are known to migrate in a CXCR2-dependent fashion toward CXCL1/CXCL8 gradients present in the tumor microenvironment (14, 15). Because T cells do not normally express CXCR2, we hypothesized that genetic modification of tumor antigen–specific T cells with the CXCR2 gene would promote their trafficking to tumor sites, thereby enhancing antitumor immune responses.

To evaluate whether CXCR2 expression in T cells enhances their tumor migration *in vivo*, we used an ultrasensitive bioluminescence imaging (BLI) system based on the detection of optimized firefly luciferase (OFL). We previously showed that BLI using OFL is sensitive enough to track fewer than 10 adoptively transferred T cells in murine models (16), and because it is noninvasive, it can allow for the evaluation of individual mice at multiple time points. Using this system, we show here that melanoma antigen–specific T cells transduced to express CXCR2 show improved migration to CXCL1 and gp100-expressing tumors. Furthermore, in two different tumor models, tumor-bearing mice treated with CXCR2-expressing T cells showed significantly improved antitumor responses and survival. These data show that enforced CXCR2 expression by tumor-specific T cells can overcome poor migration into tumor sites, thus leading to improved antitumor immune responses.

Materials and Methods

Animals and cell lines

pmel-1/Thy1.1+ T-cell receptor (TCR) transgenic mice on a C57BL/6 background were kindly provided by Dr. Nicholas Restifo (Surgery Branch, National Cancer Institute, Bethesda, MD). C57BL/6J-Tyr-2J/J albino mice were purchased from The Jackson Laboratory. All mice were maintained in a specific pathogen-free barrier facility at The University of Texas M. D. Anderson Cancer Center. Mice were handled in accordance with protocols approved by the Institutional Animal Care and Use Committee. B16 murine melanoma and MC38 murine colon adenocarcinoma cells were obtained from the National Cancer Institute. All tumor cell lines were maintained in RPMI 1640 with 10% FCS and 100 μg/mL Normocin (Invivogen).

Construction of viral vectors

Full-length murine *CXCR2* (mCXCR2; NP_034039) and m*CXCL1* (NP_032202) were amplified from the American Type Culture Collection clones by PCR. m*CXCR2* and m*CXCL1* were inserted into the pRV100 and pLV411G viral vector generated in our lab. OFL was fused with green fluorescent protein (GFP) and inserted into pRV100 vectors, as described earlier (16). Full-length human *gp100* was amplified from the WRG-gp100 vector (gift from Dr. Nicholas Restifo) and subcloned into a lentiviral vector, pLV414G. Sequences of all constructs were verified.

Retrovirus production and transduction of pmel-1 T cells

Retroviral vectors and the packaging vectors were transiently cotransfected into the packaging cell line, Plate-E, using Lipofectamine 2000 (Invitrogen) as previously described (17). Supernatants were harvested 48 hours later and concentrated between 25× and 100× using Centricon-Plus 20 tubes (Millipore). Splenocytes from pmel-1 mice were harvested and cultured in RPMI 1640 with 10% FCS, 100 μg/mL Normocin, 250 units/mL human interleukin (IL)-2 (Proleukin; Chiron), and 0.3 μg/mL anti-mouse CD3 (BD Biosciences). After 24 hours, the cells were infected with the appropriate virus in the presence of 1.6 μg/mL Polybrene (Sigma) and 2 μg/mL Lipofectamine 2000 under spin conditions at 850 × *g* for 2 hours and then incubated overnight at 37°C. The next day, fresh T-cell culture medium was added. Cells were stained with appropriate markers expressed by these viral constructs 3 days after transduction and sorted by a FACSAria (BD Biosciences).

Lentiviral transduction of tumor cells

Lentiviral vectors and packaging vectors, VSVG and Δ8.9, were cotransfected into 293 T cells using Lipofectamine 2000, and supernatant was collected after

36 hours of culture. A total of 1×10^6 tumor cells were preseeded in each well of six-well plates for 6 hours and spun at $850 \times g$ for 1 hour with 1 mL of virus supernatant and 8 μg/mL polybrene. The following day, the supernatant was removed and replaced with growth medium. Infected tumor cells were collected and sorted based on the expression of the reporter gene using FACSAria.

Immunohistochemistry

Immunohistochemistry was done on paraffin-embedded melanoma tumor tissue sections. Monoclonal antibodies against human CXCL1 (Proteintech) and CXCL8 (Santa Cruz Biotechnology) were used.

Chemotaxis assay

CXCR2-expressing or control T cells (1×10^6) were placed in 0.2 mL of complete medium in the upper chamber (3.0-μm pore size) of a well in a 24-well Transwell plate (Costar). Medium (0.4 mL) containing chemokine at various concentrations or conditioned medium from the indicated tumor cells was placed in the lower chamber, and the plates were incubated for 60 minutes at 37°C. Conditioned medium was taken from the overnight culture of 2×10^6 tumor cells in six-well plates (which contained 3 mL of medium per well). The number of cells in the lower chamber was either manually counted or, when OFL-transduced T cells were used for the migration assay, evaluated by measuring luminescence activity after the addition of D-luciferin.

Tumor reactivity assay

To test antitumor reactivity of T cells, we seeded 1×10^5 pmel-1 T cells per well in a 96-well plate and cocultured them with 1×10^4 cells from the indicated tumor lines for 16 to 18 hours. To increase the expression of MHC class I molecules, we treated B16 tumor cells with 200 ng/mL of mouse IFN-γ (BD Biosciences) overnight before the assay. T-cell responses were measured by quantifying IFN-γ in the culture supernatants by ELISA (R&D Systems), according to the manufacturer's protocols. A ^{51}Cr-release assay was used to determine the cytotoxic tumor killing by pmel-1 T cells. Tumor cells were labeled with ^{51}Cr for 1 hour and then cocultured with pmel-1 T cells at various E:T ratios. CTL activity was calculated as the percentage of specific ^{51}Cr release using the following equation: % specific killing = (sample release – spontaneous release)/(maximal release – spontaneous release) × 100%.

T-cell proliferation assay

To evaluate the effect of mCXCL1 on T-cell proliferation, we diluted anti-mouse CD3 to 5 μg/mL in PBS and used 100 μL/well to coat the bottoms of wells in a flat-bottom 96-well plate at 4°C overnight. T cells (5×10^4) were seeded into each well with or without mCXCL1 for 60 hours. [^{3}H]Thymidine was added for the last 16 hours of culture. Cells were harvested and radioactivity was counted in a scintillation counter. All experiments were done in triplicate.

Measurement of CXCL1 in cell culture supernatants

Tumor cells (2×10^6) were cultured in 3 mL RPMI 1640 with 10% FCS for 24 hours. The concentration of CXCL1 in the supernatants was determined by ELISA. Each reported value is the mean of triplicate assays.

Bone marrow–derived dendritic cells

The generation of dendritic cell (DC) from murine bone marrow cells was done as previously described (18). Briefly, bone marrow cells were grown at a starting concentration of 1×10^6 cells/mL in complete medium in the presence of 20 ng/mL granulocyte macrophage colony-stimulating factor and 100 ng/mL IL-4 (Pepro-Tech, Inc.). Fresh DC culture medium was added on days 2 and 4. Loosely adherent cells were transferred to a fresh Petri dish on day 6. The following day, nonadherent cells were resuspended in Opti-MEM (Invitrogen) at a concentration of 1×10^6 cells/mL and pulsed with 10 μmol/L H-2Db–restricted gp100 peptide (KVPRNQDWL) for 2.5 hours at 37°C. Peptide-pulsed DCs were washed three times with PBS and immediately injected into mice.

Adoptive transfer, vaccination, and treatment

C57BL/6 albino mice were s.c. implanted with either 5×10^5 B16-CXCL1 melanoma cells or 5×10^5 MC38/gp100 tumor cells (day 0). On day 6, lymphopenia was induced by administering a nonmyeloablative dose (350 cGy) of radiation. On day 7, 1×10^6 transduced pmel-1 T cells were adoptively transferred into tumor-bearing mice (n = 5-9 per group), followed by i.v. injection of 5×10^5 peptide-pulsed DCs. Recombinant human IL-2 was i.p. administered for 3 days after T-cell transfer (1.2×10^6 IU once immediately after T-cell transfer and 6×10^5 IU twice daily for the next 2 days). Tumor sizes were monitored every 2 days. Mice were sacrificed when the tumors exceeded 15 mm in diameter or when ulcers exceeded 2 mm. All experiments were carried out in a blinded, randomized fashion.

In vivo BLI

Before imaging, mice were anesthetized with isoflurane and i.p. injected with 100 μL of 20 mg/mL D-luciferin (Xenogen Corp.). After 8 minutes, animals were imaged using an IVIS 200 system (Xenogen), according to the manufacturer's manual. Living Image software (Xenogen) was used to analyze the data. Regions of interest were manually selected and quantification is reported as the average of photon flux within regions of interest. The bioluminescence signal is represented as photons/s/cm^2/sr.

Statistical analysis

The data were represented as mean ± SEM. Comparisons of differences in continuous variables between two groups were done using Student's t test. Differences in tumor size and T-cell number among different treatments were evaluated by ANOVA repeated-measures function. P values are based on two-tailed tests, with $P < 0.05$

considered statistically significant. The Kaplan-Meier test was used to compare mouse survival between groups by GraphPad Prism 5.

Results

The presence of CXCR2-cognate chemokines in the tumor microenvironment and the absence of CXCR2 on tumor-infiltrating T cells

We previously analyzed chemokine expression in freshly isolated human melanoma tumors by cDNA microarray analysis. The expression of CXCL1 and CXCL8, two CXCR2-cognate chemokines, was markedly upregulated in the tumor tissue when compared with levels in normal tissues (10). To confirm the presence of these chemokines in the melanoma tumor microenvironment, we evaluated tissue samples from melanoma patients for the expression of CXCL1 and CXCL8 by immunohistochemistry. Both chemokines were found to be present in the majority of analyzed metastatic lesions, as shown in representative photographs (Fig. 1A). Although a significant amount of CXCL1 and CXCL8 is expressed within the melanoma tumor microenvironment, very few T lymphocytes express the corresponding receptor, CXCR2. Analysis of peripheral

blood mononuclear cells (PBMC) from healthy donors and human tumor-infiltrating lymphocyte (TIL) cultures determined that <5% of CD4$^+$ or CD8$^+$ T cells express CXCR2 (Fig. 1B and C). Hence, the adoptively transferred T cells used in ACT therapy are unlikely to be capable of responding to the CXCL1/CXCL8 chemokine gradient present in the melanoma tumor microenvironment. We next explored the hypothesis that introducing the CXCR2 gene into tumor-specific T cells could enhance T-cell migration to tumor.

Establishment of a murine tumor model to monitor migration and antitumor activity of adoptively transferred T cells

Monitoring T-cell migration to tumor sites has historically been challenging due to poor sensitivity of detection, but we recently described an OFL gene that allows very low numbers of transduced murine T cells to be visualized *in vivo* (16). To further increase sensitivity of T-cell detection in these studies, we used nonpigmented, albino C57BL/6 mice and nonpigmented MC38 tumors transduced to stably express the melanoma tumor antigen gp100 (Fig. 2A). The MC38/gp100 tumor cells were recognized by gp100-specific, TCR-transgenic pmel-1
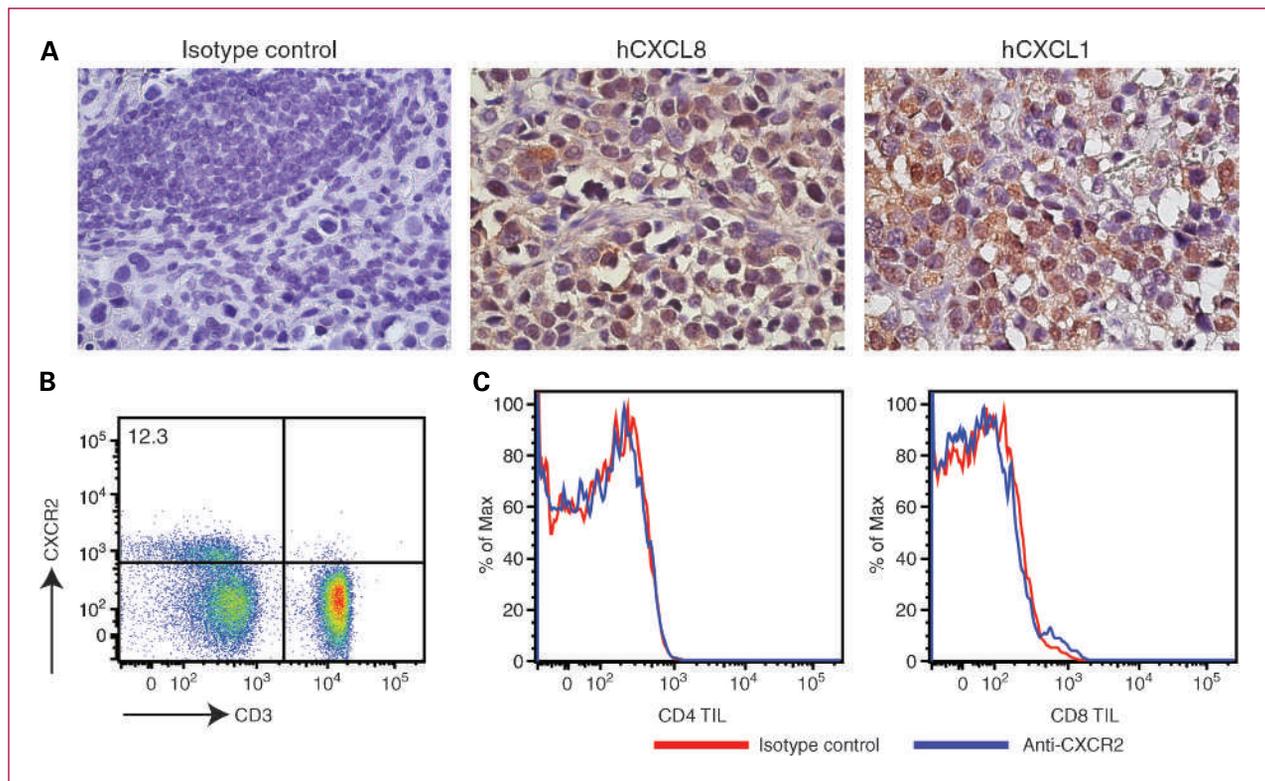

Fig. 1. Human melanoma tumors express ligands for CXCR2, but tumor-infiltrating T cells lack CXCR2 expression. A, paraffin-embedded melanoma lymph node metastases were analyzed by immunohistochemical staining for chemokine CXCL8 and CXCL1. Representative staining is shown at ×40 magnification. B, CXCR2 expression on PBMCs, as determined by flow cytometry. PBMCs from five healthy donors were stained with anti-CD3 and anti-CXCR2. C, fluorescence-activated cell sorting (FACS) analysis of CXCR2 expression on TILs. TILs isolated from four melanoma patients were stained with anti-CD4, anti-CD8, and anti-CXCR2. Representative results of all stained samples were shown.
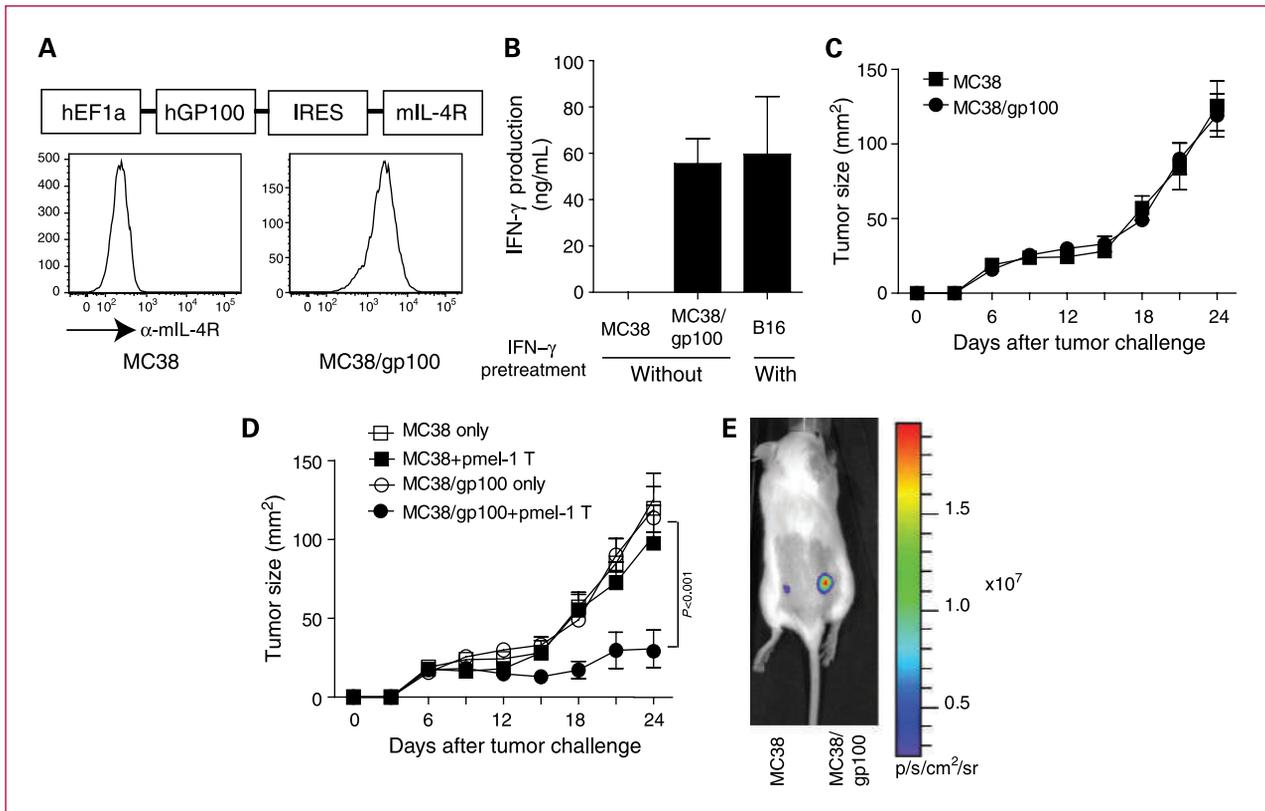
Fig. 2. Generation of gp100-expressing MC38 tumor cell lines. A, schematic representation of viral vector containing human full-length *gp100*, an internal ribosomal entry site (IRES), and the m*IL-4R* gene. The construct was transduced into MC38 cells, which were then sorted based on IL-4R expression, as shown in the right subpanel. B, IFN-γ secretion by pmel-1 T cells in response to MC38/gp100 tumors. pmel-1 T cells were cocultured with the indicated murine tumor cell lines. Twenty-four hours later, IFN-γ concentrations in the supernatants were detected by ELISA. B16 melanoma cells pretreated with IFN-γ were used as a positive control. C, growth of MC38/gp100 tumors in C57BL/6 albino mice. C57BL/6 albino mice were s.c. injected with 5×10^5 MC38 or MC38/gp100. Tumor sizes were measured every 3 d. D, treatment of MC38/gp100 tumors with pmel-1 T cells. C57BL/6 albino mice were s.c. injected with 5×10^5 MC38 or MC38/gp100. Six days later, all mice received 350 cGy irradiation. Seven days later, 5×10^6 pmel-1 T cells were transferred into tumor-bearing mice, along with 5×10^5 gp100 peptide-pulsed DC, by both i.v. injection and systemic IL-2 treatment. Tumor-bearing mice receiving irradiation only served as the control group. Tumor sizes were measured every 3 d. pmel-1 T cells suppressed the growth of MC38/gp100 tumors, but not MC38 tumors. Points, mean of five mice per group; bars, SEM. Results are representative of two experiments. E, pmel-1 T cells migrate specifically to MC38/gp100 tumors. C57BL/6 albino mice were s.c. injected with 5×10^5 MC38/gp100 in the right flank. The same number of MC38 tumor cells was implanted on the left flank. Seven days after tumor implantation, 1×10^6 sorted luciferase-expressing pmel-1 T cells were transferred to tumor-bearing mice. Six days after adoptive transfer, the intensity of luciferase signaling was measured. Data were representative of five mice.

T cells as shown by IFN-γ production and antigen-specific cytolysis *in vitro* (Fig. 2B; data not shown). Expression of gp100 did not alter the growth rate of the MC38 tumors *in vivo* (Fig. 2C) but did cause their specific recognition by adoptively transferred pmel-1 T cells, resulting in suppression of MC38/gp100 tumor growth but not that of parental MC38 tumors (Fig. 2D). More importantly, when we transferred pmel-1 T cells into mice challenged with both MC38 and MC38/gp100 on opposite flanks, the majority of pmel-1 T cells migrated to the MC38/gp100 tumor site, with few cells migrating to the MC38 tumor site (Fig. 2E). These results suggest that pmel-1 T cells specifically recognized MC38/gp100 tumor cells, and show the feasibility of monitoring the migration of tumor-specific T cells at the tumor site using luciferase imaging.

CXCR2-transduced T cells migrate specifically toward CXCL1 gradients *in vitro*

To study chemotactic migration of tumor-specific T cells, we transduced pmel-1 T cells with a retroviral vector containing the m*CXCR2* gene under the control of the murine stem cell virus long terminal repeat promoter. After retroviral transduction, >70% of the pmel-1 T cells expressed CXCR2 as measured by flow cytometry (Fig. 3A). To monitor the trafficking of transferred pmel-1 T cells *in vivo* by BLI, pmel-1 T cells were cotransduced with a retroviral vector expressing OFL-GFP. Transduced pmel-1 T cells were sorted based on positive GFP and CXCR2 expression to purities of >90% (Fig. 3B). To ensure that introduction of the *CXCR2* gene did not alter the effector function of T cells, transduced pmel-1 T cells were cocultured with parental MC38 or MC38/gp100 tumor cells, and cytokine

production and cytolytic activity were evaluated. In these assays, CXCR2-expressing pmel-1 T cells recognized and responded to cognate antigen presented by MC38/gp100 tumor cells by producing IFN-γ and mediating specific target cell killing at levels comparable with OFL-GFP–transduced control T cells (Fig. 3C and D). As expected, wild-type MC38 tumor cells failed to stimulate the activation of CXCR2-expressing pmel-1 T cells. These results showed that retroviral vector-mediated expression of CXCR2 did not alter the antigen specificity of pmel-1 T cells.

Although rodents lack a homologue to human CXCL8/IL-8, they do possess CXCL1/KC that can bind to CXCR2 and has been reported to contribute to neutrophil migration (19). Therefore, we next tested whether ectopic expression of CXCR2 in murine T cells could endow them with the capacity to respond to the cognate ligand CXCL1. Using a Transwell system, we observed that CXCR2 expression induced pmel-1 T cells to migrate specifically toward CXCL1 in a dose-dependent fashion (Fig. 4A). We also confirmed the ability of CXCR2-expressing pmel-1 T cells to migrate toward CXCL1 produced by two different murine tumor cell lines. Production of CXCL1 was robust and comparable between MC38 and MC38/gp100 tumor cells

(Fig. 4B); however, B16 melanoma tumors produced low levels of CXCL1, necessitating the establishment of a stable, CXCL1-expressing B16 tumor cell line (B16-CXCL1; Fig. 4B). As shown in Fig. 4C, conditioned medium from either MC38 or CXCL1-expressing B16 tumor cells induced enhanced migration of CXCR2-expressing pmel-1 T cells, but not control T cells, in a dose-dependent manner. By contrast, culture medium from wild-type B16 tumor cells did not increase T-cell migration, confirming that the enhanced migration was specific for CXCL1. Furthermore, the expression of CXCL1 did not alter the proliferative capacity of CXCR2-expressing pmel-1 T cells in response to specific TCR stimulation (Fig. 4D). T cells expressing CXCR2, but not control T cells, produced low levels of IFN-γ on CXCL1 stimulation. In contrast, both CXCR2-expressing and nonexpressing T cells produced similar high levels of IFN-γ when treated with both TCR stimulation and CXCL1 (Fig. 4E). Taken together, these results suggest that the introduction of the *CXCR2* gene into pmel-1 T cells enhanced their migration along a CXCL1 gradient *in vitro* in a dose-dependent manner without altering their proliferation or effector function. These results are consistent with those from our previous *in vitro* study using CXCR2-expressing human T cells (10).
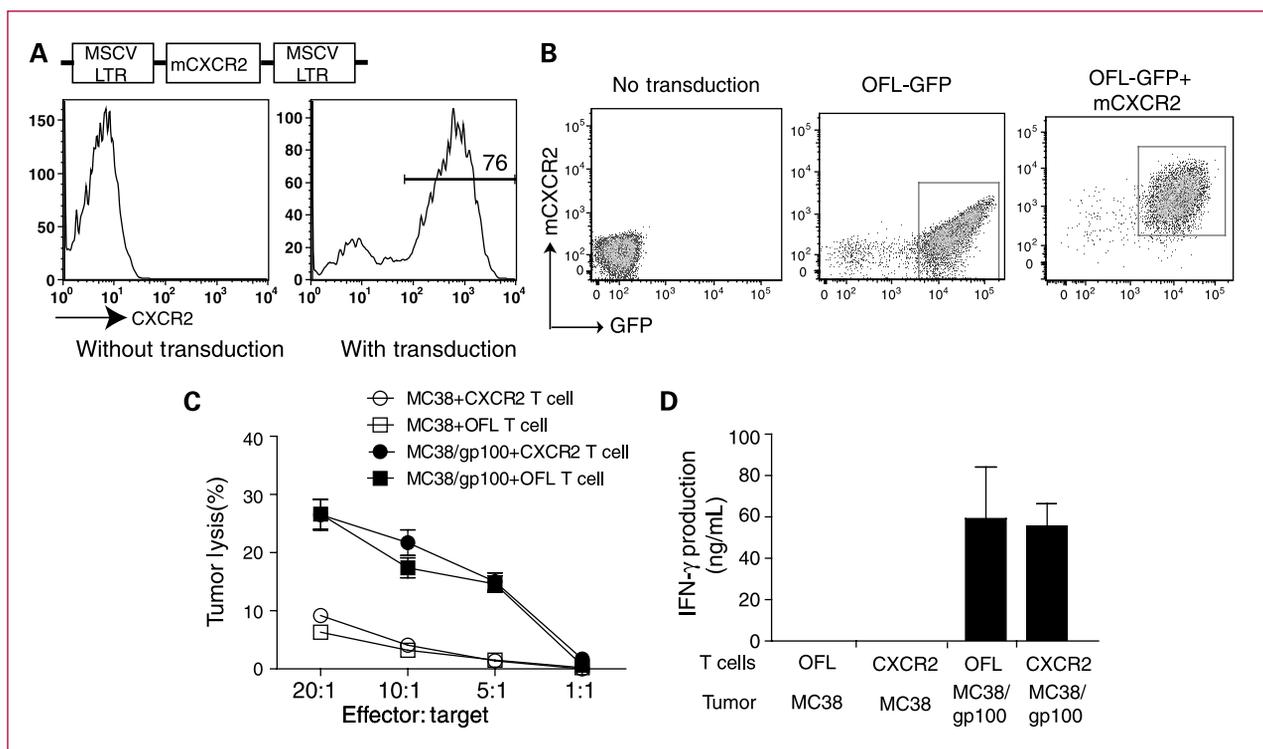

Fig. 3. Generation and functional characteristics of CXCR2-expressing pmel-1 T cells. A, schematic representation of viral vector containing mCXCR2. Long terminal repeat (LTR) from the murine stem cell PCMV virus drives high-level, constitutive expression of mCXCR2 in pmel-1 T cells. B, FACS analysis of transduced pmel-1 T cells. pmel-1 T cells were transduced with modified OFL-GFP alone or OFL-GFP and mCXCR2. Cells were sorted based on the expression of GFP or CXCR2. Sorted cells were cultured for 3 d and used for ACT. Before transfer, the purity of transferred cells was evaluated by flow cytometry. C, cytotoxic reactivity of CXCR2-expressing pmel-1 T cells against MC38/gp100 tumor. D, IFN-γ secretion by CXCR2-expressing pmel-1 T cells in response to MC38/gp100 tumors.

CXCR2-expressing T cells show enhanced trafficking to tumor *in vivo*

We next analyzed the migration of CXCR2-expressing pmel-1 cells to tumors *in vivo*. pmel-1 T cells (1×10^6) expressing OFL-GFP alone or OFL-GFP and CXCR2 were i.v. injected into C57BL/6 albino mice bearing MC38/gp100 tumors (average tumor size, 20 mm^2). Mice receiving pmel-1 T cells also received DC vaccination on the day of T-cell transfer, as well as systemic IL-2 treatment for 3 days, as described previously (Supplementary Fig. S1A; ref. 20). Luciferase intensity at the tumor site, which reflects the accumulation of adoptively transferred pmel-1 T cells, was monitored on a daily basis. Although the transferred pmel-1 T cells were detected by BLI in tumor sites as early as the second day after ACT, most of the transferred pmel-1 T cells were initially found in the lung and liver (Fig. 5A). Six days after T-cell transfer, the majority of the pmel-1 T cells were localized at the tumor site.

This pattern of distribution of transferred tumor-specific T cells is consistent with that previously reported in a murine study using a single-photon emission computed tomography fusion imaging method for T-cell detection (21). Therefore, we used the luciferase results from mice on day 6 after T-cell transfer as representative data to characterize the tumor migration of transferred pmel-1 T cells. As shown in Fig. 5B, mice that received CXCR2-expressing T cells displayed a stronger luciferase signal at the tumor site than mice that received control T cells on day 6 after T-cell transfer. The average luciferase activity in all mice ($n = 8$-9) from each group was quantified (Fig. 5C), and showed that treatment with CXCR2-expressing T cells induced more than 2-fold higher pmel-1 T-cell infiltration than mice treated with control T cells. By contrast, the percentage of pmel-1 T cells in the peripheral blood remained similar between the two groups of mice (Fig. 5D). In B16 tumors engineered to express CXCL1, we also found an
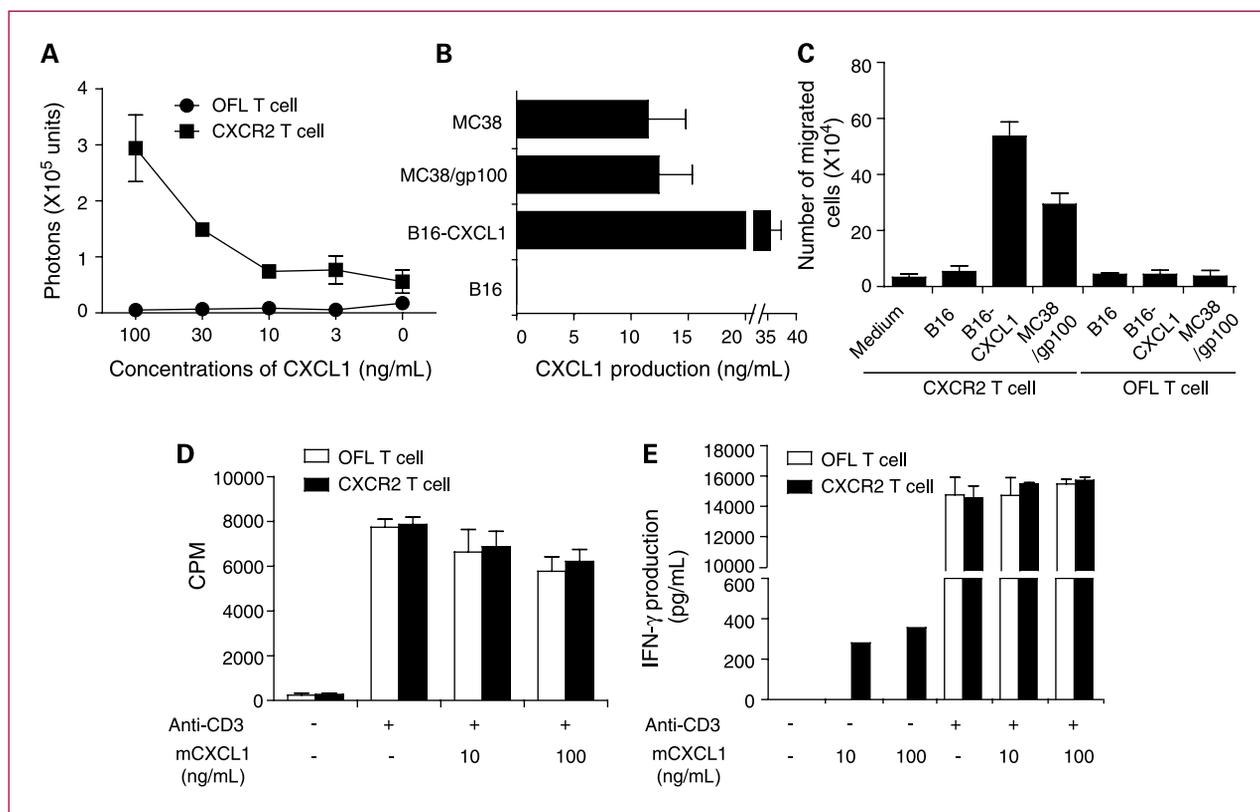

Fig. 4. Enhanced migration of CXCR2-expressing T cells along CXCL1 gradients. A, migration of CXCR2-expressing T cells along recombinant CXCL1 gradients. pmel-1 T cells were transduced with either OFL-GFP or OFL-GFP and mCXCR2 and placed into the upper wells of a Transwell system, with CXCL1 in the lower wells at the indicated concentrations. One hour later, D-luciferin was added to the lower wells. T-cell migration to the lower well was quantitated by measuring luminescent activity. B, CXCL1 production by murine tumor lines. Cells (2×10^6) from the indicated murine cell lines were plated in six-well plates; 24 h later, CXCL1 in supernatants was detected by ELISA. C, migration of CXCR2-expressing T cells along tumor cell–derived CXCL1 gradients. pmel-1 T cells were transduced with either OFL-GFP or OFL-GFP and mCXCR2 and placed into the upper wells of a Transwell system. Conditioned cell culture medium from tumor cells was loaded into the lower wells. One hour after incubation, the cell number in the lower wells was counted. D, proliferation of CXCR2-expressing pmel-1 T cells on TCR stimulation in the presence or absence of CXCL1. CXCR2- or OFL-expressing T cells were stimulated with anti-CD3 and irradiated splenocytes in the presence or absence of recombinant CXCL1. T-cell proliferation was evaluated by [^{3}H]thymidine incorporation assay. E, IFN-γ secretion by CXCR2-expressing pmel-1 T cells on TCR stimulation in the presence or absence of CXCL1. CXCR2- or OFL-expressing T cells were stimulated with anti-CD3 and irradiated splenocytes in the presence or absence of recombinant CXCL1.
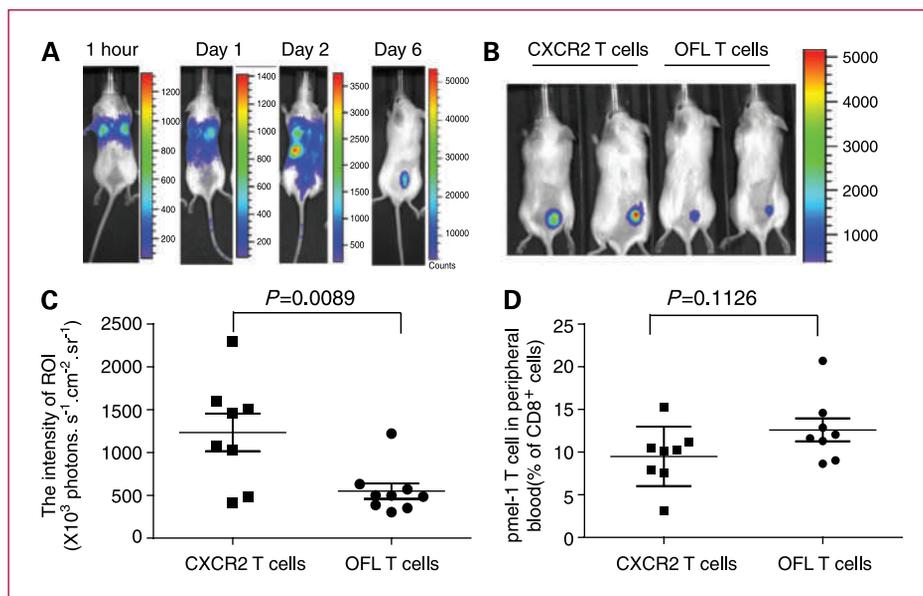
Fig. 5. Enhanced migration of CXCR2-expressing pmel-1 T cells to tumor sites. A, *in vivo* trafficking of OFL-expressing pmel-1 T cells. OFL-expressing pmel-1 T cells (1×10^6) were transferred into mice bearing established 7-d MC38/gp100 tumors. DC vaccine and IL-2 treatment were done as previously described. Imaging was done at indicated time points after T-cell transfer. B, increased accumulation of CXCR2-expressing pmel-1 T cells at the tumor site. pmel-1 T cells (1×10^6) expressing either OFL alone or CXCR2 with OFL were transferred into mice bearing established MC38/gp100 tumors. Imaging was done at day 6 after T-cell transfer. Data were from representative mice. C, quantitative imaging analysis of transferred T cells in tumor-bearing mice. Intensities of the luciferase signal at tumor sites in all tumor-bearing mice are depicted. D, percentage of Thy1.1^{+} pmel-1 T cells of the CD8^{+} T cells in the peripheral blood on day 6 after T-cell transfer. Thy1.1 is a congenic cell surface marker for transferred pmel-1 T cells. C and D, points, mean of eight mice per group; bars, SEM. Results are representative of three experiments.

increased percentage of CXCR2-expressing pmel-1 T cells at the tumor site, but not in the spleen, when compared with control T cells (Supplementary Fig. S1B). Moreover, the percentages of IFN-γ^+ pmel-1 T cells were comparable between mice receiving CXCR2-expressing T cells or control T cells, further confirming that introducing the *CXCR2* gene into tumor-specific T cells does not alter their effector function (Supplementary Fig. S1B). These results show that transduction of T cells with the *CXCR2* gene resulted in their preferential accumulation to tumor sites expressing CXCL1.

CXCR2-expressing T cells show superior antitumor activity *in vivo*

We next assessed whether CXCR2-mediated accumulation of pmel-1 T cells in tumors would result in more potent antitumor activity. Seven days after challenge with MC38/gp100 tumors, mice were treated with ACT and tumor growth was monitored. As described previously, transfer of 1×10^6 pmel-1 T cells combined with DC vaccination and IL-2 resulted in a significant decrease of MC38/gp100 tumor growth (Fig. 6A; ref. 20). More importantly, tumor growth was significantly reduced in mice receiving CXCR2-expressing pmel-1 T cells compared with mice receiving control (OFL only) pmel-1 T cells (Fig. 6A). The increased tumor suppression by CXCR2-expressing pmel-1 T cells translated into a significant increase in the survival of mice bearing MC38/gp100 tumors (Fig. 6B). In

B16-CXCL1 tumor model, tumor growth was also significantly delayed and survival was extended in mice treated with CXCR2-expressing pmel-1 T cells compared with control pmel-1 T cells (Fig. 6C and D), further corroborating our findings in a tumor model that naturally expresses gp100. CXCR2-expressing pmel-1 T cells did not confer better protection in mice bearing wild-type B16 tumors, likely due to the lack of CXCL1 expression by native B16 tumors (Fig. 6E). In the B16-CXCL1 model, tumor growth in mice receiving 1×10^6 CXCR2-expressing pmel-1 T cells was comparable with that of mice receiving 5×10^6 control pmel-1 T cells, suggesting a 5-fold increase in antitumor activity (Fig. 6F). These data support our hypothesis that enforced expression of CXCR2 in tumor-specific T cells enhances their therapeutic antitumor activity.

Discussion

Effective immunologic destruction of large and established tumors requires not only a sufficient number of activated T cells that can recognize tumor antigens with high avidity but also the ability of these cells to migrate to sites of malignancy (22). Several lines of evidence support the hypothesis that impaired tumor homing of T cells is often a rate-limiting step in antitumor immunotherapy, particularly the observation in both murine and human studies that tumors frequently continue to grow in the presence of large numbers of circulating, tumor-specific

T cells (23, 24). This point is highlighted by the disappointing clinical response rates resulting from immunization with cancer vaccines, despite the successful generation of tumor-specific T-cell reactivity *in vivo* (25). Even with ACT approaches using nonmyeloablative lymphodepletion regimens, where upwards of 75% of the circulating $CD8^+$ T cells can show antitumor activity, approximately half of metastatic melanoma patients still fail to respond to the treatment (26). Monitoring of transferred T cells has shown that the majority of infused T cells localize in the lung, liver, and spleen, whereas <1% of the total trans-

ferred T cells migrate to the tumor (5, 27). Finally, extensive T-cell infiltrates are commonly observed in tumors undergoing immunologic rejection, and the presence of such infiltrates correlates well with increased objective response rates (25). In contrast, tumors that are refractory to T-cell–based immunotherapies rarely accumulate strong immune cell infiltrates. Compared with the large number of adoptively transferred tumor-specific T cells required for effective treatment (10^{10}-10^{11}), the tumor-infiltrating T cells that presumably mediate tumor rejection *in situ* represent a small fraction of the total T cells infused (4). There
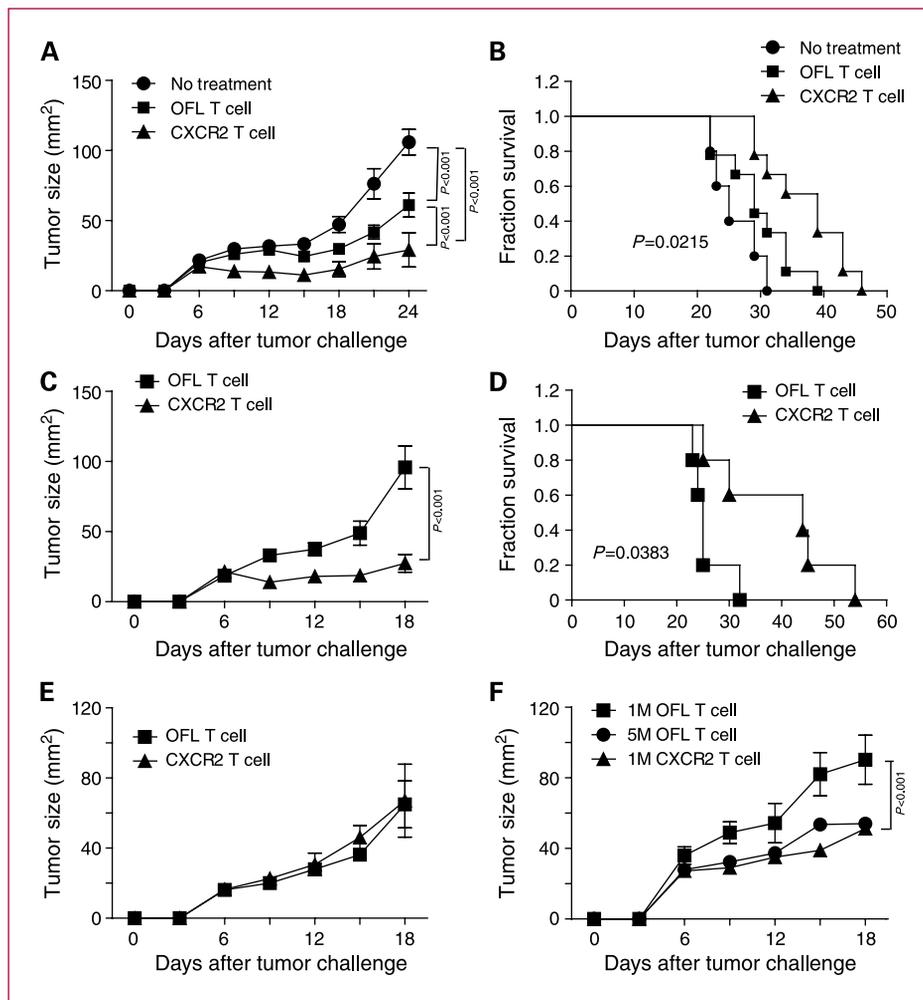

Fig. 6. Enhanced suppression of established tumors on ACT with CXCR2-expressing pmel-1 T cells. Groups of mice were implanted with 5×10^5 tumor cells on day 0, subjected to 350 cGy total body irradiation at day 6, followed on day 7 by ACT with pmel-1 T cells expressing either OFL alone or OFL and CXCR2, along with DC vaccination and systemic IL-2. A, tumor growth curve of MC38/gp100 tumor-bearing mice receiving ACT. B, Kaplan-Meier survival curves of MC38/gp100 tumor-bearing mice treated with ACT. Tumor growth curve (C) and Kaplan-Meier survival curves (D) of B16-CXCL1 tumor-bearing mice treated with ACT with CXCR2-transduced pmel-1 T cells. Tumor growth was monitored every 3 d. Points, mean; bars, SEM. *P* values in B and D were determined by two-way ANOVA. In both tumor models, CXCR2 transduction enhanced the ability of the T cells to mediate tumor regression and increased survival. Similar results were obtained in repeated experiments. In A and B, *n* = 8 to 9 for each treatment group; in C and D, *n* = 5 for each treatment group. Results are representative of two experiments. E, tumor growth curve of B16 tumor-bearing mice receiving ACT. *n* = 3 for each treatment group. F, tumor growth curve of B16-CXCL1 tumor-bearing mice receiving ACT using different numbers of OFL- or CXCR2-expressing pmel-1 T cells. Similar protocols for tumor challenge and ACT treatment were followed. Tumor-bearing mice were infused with either 1×10^6 (1M) or 5×10^6 (5M) OFL-expressing T cells, or 1×10^6 CXCR2-expressing T cells on day 7 after tumor challenge. *n* = 3 to 5 mice for each treatment group.

is also growing evidence that suggests that further proliferation of T cells *in vivo* is required for tumor trafficking and regression (20, 28, 29). Collectively, these observations strongly suggest that T-cell homing to tumors is a relatively inefficient process. Furthermore, our own unpublished data also show that clinical response to ACT positively correlates with the total number of T cells infused, suggesting that providing more cells to the tumor site may improve clinical responses.

CXCR2 is one of the G protein–coupled receptors capable of binding to both CXCL1 and CXCL8 (11). It has been shown to regulate the migration of immune effector cells. For example, Smith et al. (30) found that CXCR2 plays an important role in arresting the rolling of neutrophils to inflamed sites by using CXCR2-deficient mice. To take advantage of the high concentration of CXCL1 and CXCL8 in the tumor microenvironment, we transduced pmel-1 T cells with a viral vector expressing the mCXCR2 gene. Our results showed that the expression of CXCR2 by pmel-1 T cells enabled these cells to respond to CXCL1 gradients in the tumor but did not alter their effector functions. These results are consistent with those from our previous study using CXCR2-expressing human T cells (10). Therefore, it is possible that inducing expression of the CXCR2 gene in human tumor-specific T cells could lead these cells to migrate toward CXCL1 and CXCL8 gradients in the melanoma tumor microenvironment in patients.

To further confirm this possibility *in vivo*, we used the newly established MC38/gp100 tumor model, which allows us to monitor trafficking of transferred tumor-specific pmel-1 T cells *in vivo*. We found that tumor-specific T-cell trafficking to tumor sites was improved following CXCR2 transduction of the T cells. Enhanced trafficking of CXCR2-expressing pmel-1 T cells resulted in delayed tumor growth and extended the survival of tumor-bearing mice. Our results also suggest a positive correlation between increased migration of tumor-specific T cells to the tumor and efficacy of ACT. These findings support our hypothesis that migration of T cells to the tumor is an important and limiting factor for tumor regression in cancer patients. Because the percentage of tumor-specific T cells among the total transferred T cells in patients receiving ACT is much lower than that in most preclinical studies (e.g., almost 100% of the transferred pmel-1 T cells were tumor specific in this study), the recruitment of tumor-specific T cells into tumor sites in the clinical setting may be even more critical for the success of ACT. Therefore, we expect an enhance-

ment in antitumor immune response in patients treated with CXCR2-transduced TIL compared with patients receiving standard ACT.

Using gene-modified T cells to increase the effectiveness of ACT is challenging in cancer patients. However, this approach is feasible. Besides our own studies (31), other groups have also conducted clinical trials with genetically modified T cells. One group conducted a trial using ACT of TIL cells that had been genetically engineered to produce IL-2 and found that transferred TIL persisted better after IL-2 withdrawal (32, 33). In another clinical trial, 11 patients with neuroblastoma were infused with EBV-specific CTLs transduced with a chimeric antigen receptor that could recognize a tumor-associated antigen expressed by human neuroblastoma cells, disialoganglioside GD2. The engagement of GD2 and these genetically engineered receptors could trigger T-cell activation, and infusion of these genetically modified T cells was associated with tumor regression (34). These studies have shown that infusion of genetically modified T cells is feasible and safe and may benefit cancer patients treated with ACT.

Whereas most current strategies to genetically modify tumor-specific T cells are aimed at enhancing T-cell persistence or tumor recognition, our study focuses on an alternate strategy to increase the effectiveness of ACT by promoting T-cell homing to the tumor site. This approach may provide an important new avenue in "personalized cancer therapy" to take advantage of defined chemokine signatures within the tumor microenvironment and may further benefit cancer patients undergoing ACT. Based on the results described above, we are currently planning a clinical trial to treat melanoma patients with CXCR2-transduced TILs.

Disclosure of Potential Conflicts of Interest

No potential conflicts of interest were disclosed.

Grant Support

References

1. Dudley ME, Wunderlich JR, Yang JC, et al. Adoptive cell transfer therapy following non-myeloablative but lymphodepleting chemotherapy for the treatment of patients with refractory metastatic melanoma. J Clin Oncol 2005;23:2346–57.
2. Wrzesinski C, Paulos CM, Kaiser A, et al. Increased intensity lymphodepletion enhances tumor treatment efficacy of adoptively transferred tumor-specific T cells. J Immunother 2010;33:1–7.
3. Rosenberg SA, Dudley ME. Adoptive cell therapy for the treatment of patients with metastatic melanoma. Curr Opin Immunol 2009;21:233–40.
4. Pockaj BA, Sherry RM, Wei JP, et al. Localization of 111indium-labeled tumor infiltrating lymphocytes to tumor in patients receiving adoptive immunotherapy. Augmentation with cyclophosphamide and correlation with response. Cancer 1994;73:1731–7.
5. Fisher B, Packard BS, Read EJ, et al. Tumor localization of adoptively transferred indium-111 labeled tumor infiltrating lymphocytes in patients with metastatic melanoma. J Clin Oncol 1989; 7:250–61.
6. Pittet MJ, Mempel TR. Regulation of T-cell migration and effector

functions: insights from *in vivo* imaging studies. Immunol Rev 2008; 221:107–29.

7. Matsumura S, Wang B, Kawashima N, et al. Radiation-induced CXCL16 release by breast cancer cells attracts effector T cells. J Immunol 2008;181:3099–107.

8. Gajewski TF. Failure at the effector phase: immune barriers at the level of the melanoma tumor microenvironment. Clin Cancer Res 2007;13:5256–61.

9. Harlin H, Meng Y, Peterson AC, et al. Chemokine expression in melanoma metastases associated with CD8^{+} T-cell recruitment. Cancer Res 2009;69:3077–85.

10. Kershaw MH, Wang G, Westwood JA, et al. Redirecting migration of T cells to chemokine secreted from tumors by genetic modification with CXCR2. Hum Gene Ther 2002;13:1971–80.

11. Vandercappellen J, Van Damme J, Struyf S. The role of CXC chemokines and their receptors in cancer. Cancer Lett 2008;267:226–44.

12. Waugh DJ, Wilson C. The interleukin-8 pathway in cancer. Clin Cancer Res 2008;14:6735–41.

13. Lizee G, Cantu MA, Hwu P. Less yin, more yang: confronting the barriers to cancer immunotherapy. Clin Cancer Res 2007;13:5250–5.

14. Dirkx AE, Oude Egbrink MG, Wagstaff J, Griffioen AW. Monocyte/macrophage infiltration in tumors: modulators of angiogenesis. J Leukoc Biol 2006;80:1183–96.

15. Nardin A, Abastado JP. Macrophages and cancer. Front Biosci 2008; 13:3494–505.

16. Rabinovich BA, Ye Y, Etto T, et al. Visualizing fewer than 10 mouse T cells with an enhanced firefly luciferase in immunocompetent mouse models of cancer. Proc Natl Acad Sci U S A 2008;105:14342–6.

17. Naviaux RK, Costanzi E, Haas M, Verma IM. The pCL vector system: rapid production of helper-free, high-titer, recombinant retroviruses. J Virol 1996;70:5701–5.

18. Steinman RM, Inaba K, Turley S, Pierre P, Mellman I. Antigen capture, processing, and presentation by dendritic cells: recent cell biological studies. Hum Immunol 1999;60:562–7.

19. Czuprynski CJ, Brown JF, Steinberg H, Carroll D. Mice lacking the murine interleukin-8 receptor homologue demonstrate paradoxical responses to acute and chronic experimental infection with *Listeria monocytogenes*. Microb Pathog 1998;24:17–23.

20. Lou Y, Wang G, Lizee G, et al. Dendritic cells strongly boost the antitumor activity of adoptively transferred T cells *in vivo*. Cancer Res 2004;64:6783–90.

21. Pittet MJ, Grimm J, Berger CR, et al. *In vivo* imaging of T cell delivery to tumors after adoptive transfer therapy. Proc Natl Acad Sci U S A 2007;104:12457–61.

22. Blattman JN, Greenberg PD. Cancer immunotherapy: a treatment for the masses. Science 2004;305:200–5.

23. Peterson AC, Harlin H, Gajewski TF. Immunization with Melan-A peptide-pulsed peripheral blood mononuclear cells plus recombinant human interleukin-12 induces clinical activity and T-cell responses in advanced melanoma. J Clin Oncol 2003;21:2342–8.

24. Rosenberg SA, Sherry RM, Morton KE, et al. Tumor progression can occur despite the induction of very high levels of self/tumor antigen-specific CD8^{+} T cells in patients with melanoma. J Immunol 2005; 175:6169–76.

25. Rosenberg SA, Yang JC, Restifo NP. Cancer immunotherapy: moving beyond current vaccines. Nat Med 2004;10:909–15.

26. Rosenberg SA, Dudley ME. Cancer regression in patients with metastatic melanoma after the transfer of autologous antitumor lymphocytes. Proc Natl Acad Sci U S A 2004;101 Suppl 2:14639–45.

27. Bobisse S, Rondina M, Merlo A, et al. Reprogramming T lymphocytes for melanoma adoptive immunotherapy by T-cell receptor gene transfer with lentiviral vectors. Cancer Res 2009;69:9385–94.

28. Kjaergaard J, Peng L, Cohen PA, Shu S. Therapeutic efficacy of adoptive immunotherapy is predicated on *in vivo* antigen-specific proliferation of donor T cells. Clin Immunol 2003;108:8–20.

29. Overwijk WW, Theoret MR, Finkelstein SE, et al. Tumor regression and autoimmunity after reversal of a functionally tolerant state of self-reactive CD8^{+} T cells. J Exp Med 2003;198:569–80.

30. Smith ML, Olson TS, Ley K. CXCR2- and E-selectin-induced neutrophil arrest during inflammation *in vivo*. J Exp Med 2004;200:935–9.

31. Kershaw MH, Westwood JA, Parker LL, et al. A phase I study on adoptive immunotherapy using gene-modified T cells for ovarian cancer. Clin Cancer Res 2006;12:6106–15.

32. Liu K, Rosenberg SA. Interleukin-2-independent proliferation of human melanoma-reactive T lymphocytes transduced with an exogenous IL-2 gene is stimulation dependent. J Immunother 2003;26: 190–201.

33. Heemskerk B, Liu K, Dudley ME, et al. Adoptive cell therapy for patients with melanoma, using tumor-infiltrating lymphocytes genetically engineered to secrete interleukin-2. Hum Gene Ther 2008;19: 496–510.

34. Pule MA, Savoldo B, Myers GD, et al. Virus-specific T cells engineered to coexpress tumor-specific receptors: persistence and antitumor activity in individuals with neuroblastoma. Nat Med 2008;14:1264–70.

AACR American Association
for Cancer Research

Clinical Cancer Research

Transduction of Tumor-Specific T Cells with CXCR2 Chemokine Receptor Improves Migration to Tumor and Antitumor Immune Responses

Weiyi Peng, Yang Ye, Brian A. Rabinovich, et al.

Updated version	Access the most recent version of this article at: doi:10.1158/1078-0432.CCR-10-0712
Supplementary Material	Access the most recent supplemental material at: http://clincancerres.aacrjournals.org/content/suppl/2021/03/16/1078-0432.CCR-10-0712.DC1

Cited articles	This article cites 34 articles, 19 of which you can access for free at: http://clincancerres.aacrjournals.org/content/16/22/5458.full#ref-list-1
Citing articles	This article has been cited by 17 HighWire-hosted articles. Access the articles at: http://clincancerres.aacrjournals.org/content/16/22/5458.full#related-urls

E-mail alerts	Sign up to receive free email-alerts related to this article or journal.
Reprints and Subscriptions	To order reprints of this article or to subscribe to the journal, contact the AACR Publications Department at pubs@aacr.org.
Permissions	To request permission to re-use all or part of this article, use this link http://clincancerres.aacrjournals.org/content/16/22/5458. Click on "Request Permissions" which will take you to the Copyright Clearance Center's (CCC) Rightslink site.